

Expression of VAMP2-like Protein in Kidney Collecting Duct Intracellular Vesicles

Colocalization with Aquaporin-2 Water Channels

Søren Nielsen,* David Marples,* Henrik Birn,* Mahmood Mohtashami,† Niels Ole Dalby,§ William Trimble,‡ and Mark Knepper^{||}

*Department of Cell Biology, Institute of Anatomy, University of Aarhus, DK-8000 Aarhus, Denmark; †Department of Physiology and Centre for Research in Neurodegenerative Diseases, University of Toronto, Toronto, M5S 1A8 Canada; ‡Department of Molecular Biology, University of Aarhus, DK-8000 Aarhus, Denmark; and ^{||}Laboratory of Kidney and Electrolyte Metabolism, National Heart, Lung, and Blood Institute, National Institutes of Health, Bethesda, Maryland 20892

Abstract

Body water balance is controlled by vasopressin, which regulates Aquaporin-2 (AQP2) water channels in kidney collecting duct cells by vesicular trafficking between intracellular vesicles and the plasma membrane. To examine the molecular apparatus involved in vesicle trafficking and vasopressin regulation of AQP2 in collecting duct cells, we tested if targeting proteins expressed in the synaptic vesicles, namely vesicle-associated membrane proteins 1 and 2 (VAMP1 and 2), are expressed in kidney collecting duct. Immunoblotting revealed specific labeling of VAMP2 (18-kD band) but not VAMP1 in membrane fractions prepared from kidney inner medulla. Controls using preadsorbed antibody or preimmune serum were negative. Bands of identical molecular size were detected in immunoblots of brain membrane vesicles and purified synaptic vesicles. VAMP2 in kidney membranes was cleaved by tetanus toxin, revealing a tetanus toxin-sensitive VAMP homologue. Similarly, tetanus toxin cleaved VAMP2 in synaptic vesicles. In kidney inner medulla, VAMP2 was predominantly expressed in the membrane fraction enriched for intracellular vesicles, with little or no VAMP2 in the plasma membrane enriched fraction. This was confirmed by immunocytochemistry using semithin cryosections, which showed mainly vesicular labeling in collecting duct principal cells, with no labeling of intercalated cells. VAMP2 immunolabeling colocalized with AQP2 labeling in intracellular vesicles, as determined by immunoelectron microscopy after double immunolabeling of isolated vesicles. Quantitative analysis of 1,310 vesicles revealed a highly significant association of both AQP2 and VAMP2 in the same vesicles ($P < 0.0001$). Furthermore, the presence of AQP2 in vesicles immunisolated with anti-VAMP2 antibodies was confirmed by immunoblotting. In conclusion, VAMP2, a component of the neuronal SNARE complex, is expressed in vesicles carrying AQP2, suggesting a role in vasopressin-regulated vesicle trafficking of AQP2 water channels. (*J. Clin. Invest.* 1995. 96:1834–1844.) **Key**

words: vasopressin • vesicular trafficking • tetanus toxin • immunoelectron microscopy

Introduction

The antidiuretic hormone, vasopressin, controls body water balance by regulating Aquaporin-2 (AQP2),¹ the predominant vasopressin-regulated water channel in the kidney collecting duct (for review see reference 1). AQP2 (2) is abundant in both plasma membrane and intracellular vesicles of collecting duct principal cells (3–6). Mutations in the AQP2 gene cause severe diabetes insipidus in humans (7) and both lithium-induced nephrogenic diabetes insipidus (8) and central diabetes insipidus (4) in rats and are associated with markedly reduced levels of AQP2 expression in parallel with severe polyuria. A long-standing question has been how vasopressin acutely regulates collecting duct water permeability and body water balance. We have shown recently that acute stimulation with vasopressin induces a translocation of AQP2 water channels from intracellular vesicles to the apical plasma membrane, in parallel with an increase in the osmotic water permeability in isolated perfused collecting ducts (6). This provided the first direct evidence that trafficking of AQP2 water channels represents the regulatory mechanism for the hydroosmotic action of vasopressin. We have subsequently confirmed this by *in vivo* studies (5). Based on these studies it became important to define the molecular apparatus involved in the specific targeting, and regulation of targeting, of vesicles carrying AQP2 water channels. Such targeted delivery requires a set of signals to ensure that vesicles containing AQP2 are transported to, and fuse specifically with, the apical plasma membrane. Furthermore, the delivery process must be regulated, so that vesicle fusion, and hence AQP2 insertion into the plasma membrane, only occurs when the cells are exposed to the hormonal trigger.

Recently the SNARE hypothesis, describing a protein assembly–disassembly pathway, was proposed for vesicle trafficking including the sequential steps of synaptic vesicle docking, activation, and fusion. The SNARE hypothesis (9, 10) proposes that vesicles and their target plasma membrane are

Address correspondence to Søren Nielsen, M.D., Ph.D., Department of Cell Biology, Institute of Anatomy, University of Aarhus, DK-8000 Aarhus C, Denmark. Phone: 45–8942–3046; FAX: 45–8619–8664; E-mail: SN@ANA.AAU.DK

Received for publication 22 February 1995 and accepted in revised form 16 June 1995.

The Journal of Clinical Investigation, Inc.
Volume 96, October 1995, 1834–1844

1. *Abbreviations used in this paper:* AQP2, Aquaporin-2 water channel protein; NSF, *N*-ethylmaleimide-sensitive fusion protein; SNAP, soluble NSF attachment protein; SNAP25, synaptosomal-associated protein of 25 kD; SNARE, SNAP receptor; TeTx L, tetanus toxin light chain 1; t-SNARE, SNAP receptor on the cognate target membrane; VAMP, vesicle-associated membrane protein; v-SNARE, vesicle-associated SNARE.

each associated specifically with one member of a pair of membrane proteins, the soluble *N*-ethylmaleimide-sensitive fusion protein (NSF) attachment protein (SNAP) receptors. The vesicle-associated SNAP receptor (v-SNARE) is thought to pair with a SNAP receptor on the cognate target membrane (t-SNARE) before assembly with SNAPs and NSF into a fusion particle (10). This process is thought to mediate the specific targeting and fusion of the vesicle to its acceptor membrane. Three synapse membrane proteins have been extensively characterized and later were found to be SNAREs (9). The vesicle-associated membrane protein (VAMP), or synaptobrevin (11–13), is a v-SNARE, whereas syntaxin (14, 15) and SNAP25 (16) are t-SNAREs (9). Three mammalian isoforms of VAMP have been characterized and sequenced, VAMP1 (11), VAMP2 (11, 12, 17), and cellubrevin (18). VAMP2 and cellubrevin are substrates for clostridial toxins including tetanus toxin (19), whereas VAMP1 of rat is tetanus toxin resistant. The VAMP homologues are also differentially expressed. VAMP1 is believed to be primarily expressed in neuronal cells (20), whereas VAMP2 is abundantly expressed in neuronal cells and in certain nonneuronal tissues (21, 22). Thus, neuronal and nonneuronal cells may share similar molecular vesicle targeting mechanisms for regulated exocytosis. In this study we investigate whether elements of the vesicle targeting proteins, namely the VAMPs, are expressed in the renal collecting duct, using immunoblotting, membrane fractionation, tetanus toxin treatment, vesicle immunoisolation, immunocytochemistry, and quantitative immunoelectron microscopy. In particular, we have studied intracellular vesicles containing AQP2, the vasopressin-regulated water channel, to investigate the mechanisms involved in the targeting and regulation of water channel delivery in response to vasopressin. We demonstrate that AQP2-bearing vesicles contain VAMP2, a component of the SNARE complex, suggesting that VAMP2 is involved in vasopressin-regulated targeting of AQP2.

Methods

Antibodies

The antibodies recognizing VAMP1 and VAMP2 have been described previously (12, 21, 23). Peptides corresponding to amino acids 1–14 of rat VAMP-1 and 1–16 of rat VAMP-2 were synthesized with the addition of a cysteine residue at the carboxyl terminus. These were conjugated to inject maleimide-activated bovine serum albumin (Pierce, Rockford, IL) and were used to immunize rabbits. In addition, an anti-VAMP antibody recognizing a conserved region of VAMP was prepared in the same way using a synthetic peptide corresponding to amino acids 50–65 of VAMP2 (a conserved region), and the antibody recognizes both VAMP1 and VAMP2. Crude antisera were affinity purified by passing immune serum over Sulfolink coupling columns (Pierce) to which the peptides had been conjugated. The columns were washed with 20 column volumes of each of the following buffers in order: PBS; 2 M NaCl in 10 mM phosphate, pH 7.0; 0.1 M sodium borate, pH 9.1; and finally with 0.15 M NaCl in phosphate, pH 4.5. Affinity-purified antibodies were then eluted in 2 column volumes of 20 mM glycine-HCl, pH 2.5, and immediately buffered to neutrality with an equal volume of 50 mM Tris, pH 8.5. Preimmune serum, immune serum, or affinity-purified antibody was used for immunoblotting and immunolabeling. For immunolabeling of AQP2, immune serum or affinity-purified antibody was used, which has been characterized in detail previously (3, 4, 6, 8). This antibody was raised in rabbit against a synthetic peptide corresponding to the COOH-terminal 22 amino acids of AQP2.

Preparation of membrane vesicles and subcellular fractionation

Crude membrane fraction of kidney inner medulla. The inner medulla was dissected from each kidney, minced finely, and homogenized in 10 ml of dissecting buffer (0.3 M sucrose, 25 mM imidazole, 1 mM EDTA, pH 7.2, and containing the following protease inhibitors: 8.5 μ M leupeptin and 1 mM PMSF), with five strokes of a motor-driven Potter-Elvehjem homogenizer at 1,250 rpm. This homogenate was centrifuged (L8M centrifuge; Beckman Instruments, Inc., Fullerton, CA) at 4,000 g for 15 min at 4°C. The pellet was rehomogenized with three to five strokes, and centrifugation was repeated to increase yields. The supernatants were pooled and centrifuged at 200,000 g for 1 h. The resultant pellet was resuspended in \sim 100 μ l of dissecting buffer and assayed for protein concentration using the method of Lowry (see reference 25).

Subcellular fractionation of kidney inner medulla. Membrane vesicle fractions were prepared as previously described (5), using a standard preparatory method for membrane fractions from kidney (24). Briefly, finely minced kidney inner medulla was homogenized as described above. This homogenate was centrifuged at 4,000 g for 15 min. The supernatant was collected, and the pellet was rehomogenized in fresh buffer with three strokes of the homogenizer, and centrifugation was repeated. The supernatants were pooled, and low speed and high speed vesicle fractions were prepared consecutively by centrifugation of the supernatant at 17,000 g for 30 min and 200,000 g for 1 h, respectively. These represented fractions enriched for plasma membrane (low speed) and intracellular vesicles (high speed). The pellets were resuspended in dissecting buffer and were assayed for protein concentration using the method of Lowry (25).

Preparation of brain membrane vesicles and purified synaptic vesicles. Crude membranes of whole rat brains (250-gram Wistar rats) were prepared as described above. Synaptic vesicles were prepared by gradient centrifugation according to the methods described by Huttner et al. (26). Cerebral cortexes were obtained from decapitated newborn rats (Wistar). The cortexes were homogenized in 0.32 M sucrose in 4 mM Hepes-NaOH buffer, pH 7.3, and the homogenate was centrifuged at 1,000 g for 15 min. The supernatant was then spun at 1,000 g for 15 min followed by a second centrifugation at 10,000 g for 15 min to obtain a synaptosome fraction. The synaptosome pellet was resuspended in buffered sucrose and disrupted by hypoosmotic shock. After centrifugation at 25,000 g for 20 min, the supernatant was centrifuged at 165,000 g for 2 h to obtain a synaptic vesicle-enriched fraction.

Electrophoresis and immunoblotting

The membrane samples were solubilized in Laemmli sample buffer containing 2.5% SDS. Samples were loaded at 10–100 μ g/lane onto 15% SDS-PAGE gels, run on a minigel system (Bio Rad Laboratories, Hercules, CA), and proteins were transferred to nitrocellulose paper by electroelution. The blots were blocked for 1 h with 5% skimmed milk in PBS-T (80 mM Na₂HPO₄, 20 mM NaH₂PO₄, 100 mM NaCl, 0.1% Tween 20, pH 7.5) and then washed with PBS-T. The blots were then incubated overnight at 4°C with antibody in PBS-T with 0.1% BSA at the following dilutions: anti-VAMP2 immune serum (1:1,000); affinity-purified anti-VAMP2 (0.3 μ g IgG/ml); anti-VAMP1 immune serum (1:500) or affinity-purified anti-VAMP1 (0.6 μ g IgG/ml). After washing, the blots were incubated for 1 h with horseradish peroxidase-conjugated goat anti-rabbit secondary antibody (P448; DAKO, Copenhagen, Denmark) (1:3,000). After final washing, antibody binding was visualized using the ECL system (enhanced chemiluminescence; Amersham International, Buckinghamshire, United Kingdom). Controls using preimmune serum, anti-VAMP2 serum preadsorbed with excess synthetic peptide (conjugated to inject maleimide-activated bovine serum albumin), or omission of primary or secondary antibody revealed no labeling.

For AQP2, low speed (plasma membrane-enriched) and high speed (intracellular vesicle-enriched) membrane fractions (5 μ g/lane) were loaded on 12% SDS-PAGE gels, electrophoresed, and immunoblotted with anti-AQP2 antibody as described previously (3, 4, 6, 8).

VAMP2 proteolysis with tetanus toxin

Whole tetanus toxin. Purified clostridium tetanus toxin (lot 60) was kindly provided by Statens Seruminstitut (Copenhagen, Denmark). The tetanus toxin preparation was incubated with 10 mM DTT for 30 min at 22°C before use to ensure complete reduction. Membrane fractions from kidney inner medulla, brain, and synaptic vesicles were divided into thirds and treated for 60 min at 37°C either with: the DTT-treated toxin (toxin concentration at 0.4 Lf/ μ l); PBS; or tetanus toxin boiled for inactivation. The samples were finally solubilized in Laemmli sample buffer to give 2.5% SDS.

Recombinant tetanus toxin light chain. Recombinant tetanus toxin light chain 1 (TeTx L) containing a COOH-terminal His⁶ tag in Qiagen Express plasmid pQE3 (kindly provided by H. Niemann; Tubingen, Germany) was expressed in *Escherichia coli* and purified by binding to ProBond Ni-charged Sepharose resin (Invitrogen, San Diego, CA) according to the protocols of the manufacturer. TeTx L chains were concentrated by ultrafiltration (centricon-3 concentrators; Amicon, Inc., Beverly, MA) before use. Protein concentrations were determined according to the assay of Bradford. Purified TeTx L chain was incubated for 2 h at room temperature in 10 mM DTT before addition to protein samples. A final concentration of 500 nM TeTx L chain was added to membrane fractions containing 15 μ g of total protein in 100 mM NaCl, 20 mM Hepes, pH 7.4, in the presence of 0.1% Triton X-100 and an additional 1 mM DTT. The samples were incubated for 1 h at 37°C and the reaction was stopped by the addition of SDS to 1%.

Vesicle isolation with anti-VAMP2 antibodies

Protein A-purified polyclonal anti-VAMP2 antibodies were biotinylated according to instructions using a commercial kit (ImmunoPure®; Pierce). This involves incubating 7.5 mg of purified immunoglobulin with 275 μ l of NHS-LC-biotin (1 mg/ml) for 2 h at 5°C in 0.01 M PBS with 0.15 M NaCl, pH 8.5. Unreacted biotin was removed by extensive dialysis for 24 h in PBS. For vesicle immunoisolation, the membrane fraction enriched for intracellular vesicles from kidney inner medulla (see above and reference 5) was used. 85 μ l of intracellular membrane vesicles (1 mg/ml) was incubated overnight at 5°C with 3.2 mg biotinylated anti-VAMP2 antibody. Avidin-agarose beads (1.5 ml) (Calbiochem-Novabiochem Corp., La Jolla, CA), washed three times in 0.01 M PBS with 0.15 M NaCl, were used for extraction. The beads were added to the membrane solution and incubated overnight at 5°C. Beads were then recovered and washed four times in 0.01 M PBS with 0.15 M NaCl by careful centrifugation at 100 g. Proteins were eluted using Laemmli's sample buffer and recovered in the supernatant after centrifugation at 14,000 g. Recovered material was analyzed by immunoblotting using anti-AQP2 antibody.

Immunocytochemistry

Immunocytochemistry was performed as described previously (3, 27–29). Rat kidneys (from Wistar rats of 250 grams allowed free access to food and water) were perfusion fixed by retrograde perfusion through the abdominal aorta with 8% paraformaldehyde in 0.1 M sodium cacodylate buffer, pH 7.2. Tissue blocks prepared from the kidney inner medulla were postfixed in the same fixative for 2 h, infiltrated for 30 min with 2.3 M sucrose (30) containing 2% paraformaldehyde, mounted on holders, and rapidly frozen in liquid nitrogen. Semithin cryosections (0.85 μ m) were obtained with a cryoultramicrotome (Reichert Jung, Vienna, Austria), and the sections were placed on gelatin-coated glass slides. After preincubation with PBS containing 1% BSA and 0.05 M glycine, the sections were incubated with anti-VAMP antibodies (described above). Antibodies were used at the following concentrations: affinity-purified anti-VAMP2 (1 μ g IgG/ml); affinity-purified anti-VAMP (1 μ g IgG/ml), affinity-purified anti-VAMP1 (1 μ g IgG/ml). The labeling was visualized by use of horseradish peroxidase-conjugated secondary antibody (P448, 1:100; DAKO). Sections were counterstained with Meier counter stain. The following controls were performed: (a) incubation with protein A-purified rabbit IgG instead of primary antibody; (b) adsorption controls, made by preincubating

the affinity-purified antibodies with excess of BSA-conjugated peptide; and (c) incubation without use of primary antibody or without primary and secondary antibody. All controls revealed absence of labeling.

Immunoelectron microscopy of isolated vesicle fractions

Enriched intracellular vesicles from inner medulla, crude brain membrane vesicles, and purified synaptic vesicles were used at 0.1–0.5 μ g/ μ l. The vesicle fractions (2 μ l) were applied to newly negative-glowed carbon film supported by 300 mesh nickel grids (Graticules Ltd, Tonbridge, Kent, England). After 2 min, excess fluid was removed and the grids were floated on drops of PBS and rinsed twice. Subsequently the grids were preincubated for 5 min with PBS containing either 0.1% defatted milk or 0.1% BSA, and then rinsed twice in PBS. After incubation with primary antibody (as described above) for 30 min at room temperature, the labeling was visualized with goat anti-rabbit IgG conjugated to 10-nm colloidal gold particles (BioCell Research Laboratories, Cardiff, United Kingdom) or with protein A conjugated to 10-nm colloidal gold particles (BioCell Research Laboratories). Double immunolabeling for AQP2 and VAMP2 was done by a sequential immunolabeling procedure with a blocking step in between. Grids were first immunolabeled with affinity-purified anti-AQP2 (0.1–0.8 μ g IgG/ml) and the labeling was visualized with protein A conjugated to 10-nm colloidal gold particles. Subsequently, the grids were incubated with excess protein A (0.1 mg/ml) for 15 min to block free binding sites. Then the immunolabeling was repeated with affinity-purified anti-VAMP2 (1 μ g IgG/ml) which was then visualized with protein A conjugated to 5-nm colloidal gold particles (Amersham International). In parallel experiments, labeling was done first for VAMP2 and then for AQP2. The grids were finally rinsed with PBS with 10 mM imidazole (pH 7.4) and negatively stained with 1% uranyl acetate. Grids were analyzed in Philips CM100 or Philips EM208 electron microscopes.

Quantification of AQP-2 and VAMP2 double immunolabeling in intracellular vesicle fraction. Electron micrographs were taken and printed at a final magnification of 75,000. 1,310 vesicles were analyzed and the double labeling was quantified in four groups: (a) vesicles labeled only for VAMP2, (b) vesicles labeled only for AQP2, (c) vesicles labeling both for AQP2 and VAMP2, or (d) vesicles without any label. The number of vesicles within the four groups was determined and the number of gold particles was counted and densities were presented as means \pm SE. The double labeling pattern was analyzed statistically by a χ^2 test.

Results

VAMP2 expression in kidney inner medulla. Body water balance is controlled by vasopressin, which regulates AQP2 in kidney collecting duct by vesicular trafficking (6). To examine the molecular apparatus involved in regulated trafficking of AQP2, we tested if VAMP homologues are expressed in kidney collecting duct. SDS gel electrophoresis and immunoblotting were performed using membrane preparations from kidney inner medulla and from brain included as a positive control (Figs. 1–3). As shown in Fig. 1, a distinct 18-kD band is seen in crude membrane preparations of whole brain (lanes 1 and 7) and in a membrane preparation enriched for synaptic vesicles (lanes 2 and 5) when probed with the antibody against VAMP2. This is consistent with the molecular mass of VAMP2 (11–13). Immunoblots of membranes from dissected kidney inner medullae reveal an identical comigrating 18-kD band (Fig. 1, lanes 3 and 6), demonstrating the presence of VAMP2 or a VAMP2-like homologue in kidney inner medulla. Controls reveal an absence of labeling in brain and inner medullary membrane vesicles (Fig. 1, middle). Use of affinity-purified anti-VAMP2 (see below) or an affinity-purified polyclonal antibody, which recognizes a conserved region of VAMP1 and VAMP2

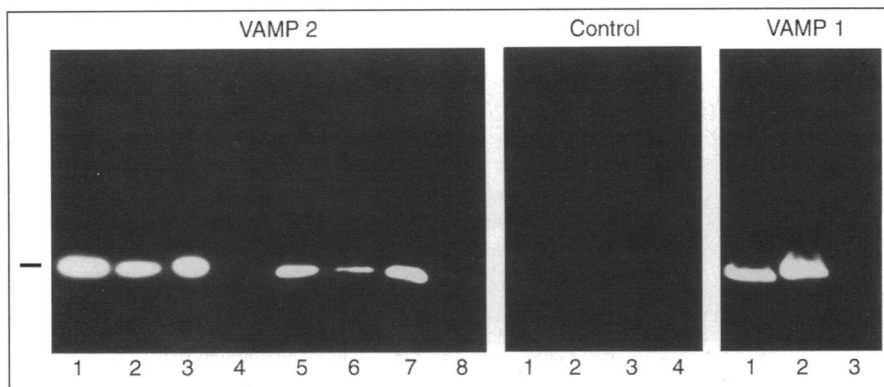


Figure 1. Immunoblots of membrane preparations from rat kidney inner medulla and brain. SDS-PAGE was run using 15% polyacrylamide gels. The left panel shows a crude membrane fraction of whole brain (20 and 10 μ g, lanes 1 and 7); purified synaptic vesicles (20 and 10 μ g, lanes 2 and 5); membrane fraction of kidney inner medulla from two different rats (100 and 50 μ g, lanes 3 and 6); inner medulla homogenate (100 μ g, lane 4) and crude membrane fraction from kidney cortex (100 μ g, lane 8) were applied in the respective lanes. Immunoblots were reacted with anti-VAMP2 serum (1:1,000). The bar indicates the 18-kD band. The middle panel shows the crude membrane fraction

of whole brain (20 μ g, lane 1); purified synaptic vesicles (20 μ g, lane 2); membrane fraction of kidney inner medulla (100 μ g, lane 3) and kidney inner medulla homogenate (100 μ g, lane 4). Immunoblot was reacted with preimmune serum (1:1,000). The right panel shows the crude membrane fraction of whole brain (20 μ g, lane 1), purified synaptic vesicles (20 μ g, lane 2), or membrane fraction of kidney inner medulla (100 μ g, lane 3). Immunoblot was reacted with affinity-purified anti-VAMP1 (0.8 μ g IgG/ml).

(not shown), demonstrated an identical 18-kD band. In contrast, an affinity-purified antibody specific for VAMP1 revealed no immunoreactivity in membranes from kidney inner medulla, whereas heavy VAMP1 expression was detected in brain membranes and synaptic vesicles (Fig. 1, right). This further supports the conclusion that VAMP immunoreactivity in kidney inner medulla represents VAMP2 or a closely related homologue.

Tetanus toxin treatment of VAMP2. Three series of experiments were performed to document and characterize the expression of VAMP2 in kidney inner medulla: tetanus toxin treatment (Fig. 2), immunoblotting of subcellular fractions of kidney inner medullary membranes (Fig. 3), and immunocytochemistry and immunoelectron microscopy (Figs. 4–8). Tetanus toxin has been shown to hydrolyze specifically VAMP2 in brain and synaptic vesicles, leaving VAMP1 intact (19, 31). As shown in Fig. 2, treatment with purified whole tetanus toxin cleaved VAMP2 in crude membrane vesicles of brain. A weak band of

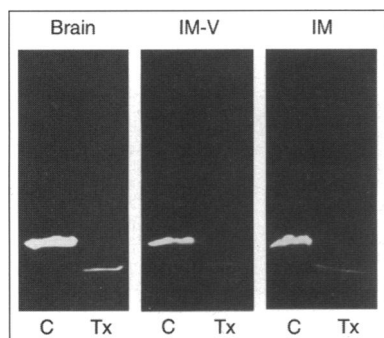


Figure 2. Immunoblots of membrane fractions from brain and kidney inner medulla treated with purified whole tetanus toxin (Tx) or phosphate buffered saline as control (C). SDS-PAGE was run using 15% polyacrylamide gels. Crude membrane fractions from rat brain (Brain, 20 μ g/lane), membrane fraction from kidney inner

medulla enriched for intracellular vesicles (IM-V, 100 μ g/lane), or a crude membrane fraction from kidney inner medulla (IM, 150 μ g/lane) was used. Immunoblots were reacted with affinity-purified anti-VAMP2 (0.3 μ g IgG/ml). In nontreated controls the 18-kD VAMP2 band is present. After tetanus toxin cleavage, the 18-kD VAMP2 is absent. VAMP2 was completely cleaved with no intact VAMP2 left, whereas an \sim 12-kD hydrolysis product was detectable. The fragment of \sim 12 kD was barely detectable as described previously (37), due to reduced ability of the fragments to bind the nitrocellulose membrane during blotting.

\sim 12 kD, the predicted size of the hydrolysis product (19), was detectable, whereas no intact VAMP2 remained. Treatment of kidney inner medullary membranes with whole tetanus toxin also resulted in cleavage of VAMP2 (Fig. 2). Toxin treatment of both a membrane preparation enriched for intracellular vesicles or a crude membrane fraction of kidney inner medulla revealed cleavage of VAMP2. These results further support the conclusion that the VAMP homologue expressed in the kidney inner medulla is VAMP2 or a VAMP2-like protein. Parallel experiments performed with a recombinant light chain tetanus toxin preparation gave identical results, with total cleavage of VAMP2 in membranes from kidney inner medulla and brain (data not shown). Control experiments with tetanus toxin inactivated by boiling (not shown) or with PBS instead of toxin at otherwise identical experimental conditions revealed intact VAMP2 in both brain and kidney membrane preparations (18-kD band, Fig. 2).

VAMP2 is predominantly expressed in intracellular vesicles in inner medullary collecting duct. A protocol for subcellular fractionation of kidney inner medullary membranes has been described previously in detail (see Methods). Two fractions were obtained, one enriched for intracellular vesicles (the high speed pellet) and one enriched for plasma membranes (the low speed pellet). AQP2 has been shown previously to be expressed heavily both in the plasma membrane and in intracellular vesicles (3). Immunoblotting, shown in Fig. 3, confirms abundant AQP2 in both fractions (Fig. 3, A, compare lanes 1 and 2). In contrast, immunoblotting revealed that VAMP2 is predominantly expressed in the fraction enriched for intracellular vesicles (Fig. 3, B, lane 1), whereas very little or no VAMP2 was present in the fraction enriched for plasma membranes (Fig. 3, B, lane 2). Controls using anti-VAMP2 previously reacted with the immunizing VAMP2 peptide revealed no labeling (Fig. 3, B). Thus, the VAMP2 immunoreactivity in kidney inner medulla is predominantly expressed in the fraction enriched for intracellular vesicles.

To further characterize the cellular and subcellular localization of VAMP2 in kidney, thin cryosections (0.85 μ m) of kidney inner medulla were subjected to immunolabeling with antibodies against VAMP2. Distinct labeling was observed of inner medullary collecting duct principal cells (Fig. 4, a and b), whereas intercalated cells were unlabeled (Fig. 4 b, heavy

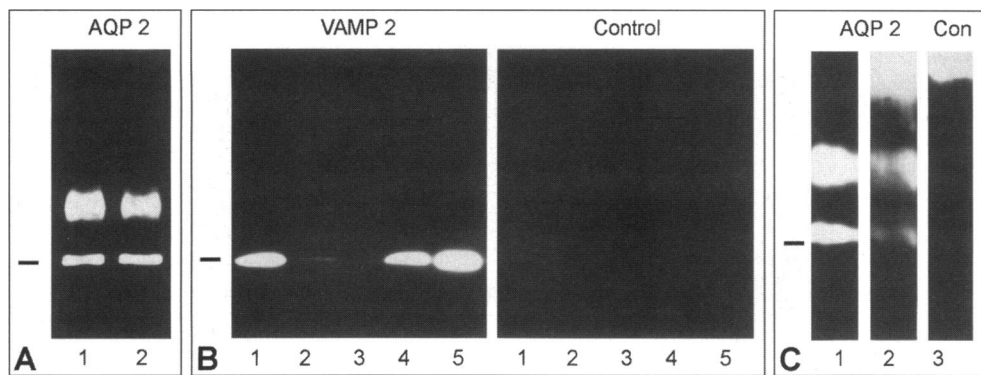


Figure 3. Immunoblots of subcellular membrane fractions from rat kidney inner medulla reacted either with anti-VAMP2 (*VAMP2*), preadsorbed anti-VAMP2 (*Control*), or anti-AQP2 (*AQP2*). (**A**) Membrane fractions enriched for intracellular vesicles (5 μ g, lane 1) or enriched for plasma membranes (5 μ g, lane 2) were applied in each lane, electrophoresed into 12% polyacrylamide gels, and immunoblotted with anti-AQP2 serum diluted 1:1,500. Heavy expression of both nonglycosylated

(28-kD band is indicated by the bar) and glycosylated AQP2 (upper band) was detected in both membrane fractions. (**B**) Membrane fractions (20 μ g) or purified synaptic vesicles (20 μ g) were applied in lanes 4 and 5, respectively, whereas lane 3 is empty. The membranes were electrophoresed into 15% polyacrylamide gel slabs and immunoblotted with anti-VAMP2 serum diluted 1:1,000. VAMP2 in kidney membranes comigrates with VAMP2 in brain (lane 4) and synaptic (lane 5) vesicles at 18 kD (18 kD is indicated by the bar). The control panel is identical to the VAMP2 panel, except that it was probed with anti-VAMP2 previously preadsorbed with excess immunizing peptide. (**C**) Membrane fractions enriched for intracellular vesicles (5 μ g, lane 1) or anti-VAMP2 immunisolated vesicles from a fraction enriched for intracellular vesicles (lanes 2 and 3) were applied in each lane, electrophoresed into 15% polyacrylamide gels, and immunoblotted with anti-AQP2 serum diluted 1:1,500 (*AQP2*). Significant labeling of both nonglycosylated (the 28-kD band is indicated by the bar) and glycosylated AQP2 (upper band) was detected in VAMP-2 isolated vesicles (lane 2), whereas control labeling using anti-AQP2 previously reacted with immunizing peptide (*Con*) revealed absence of labeling (lane 3). IgG, from the immunoprecipitation process, is recognized by the secondary antibody, as seen on the upper part of lanes 2 and 3.

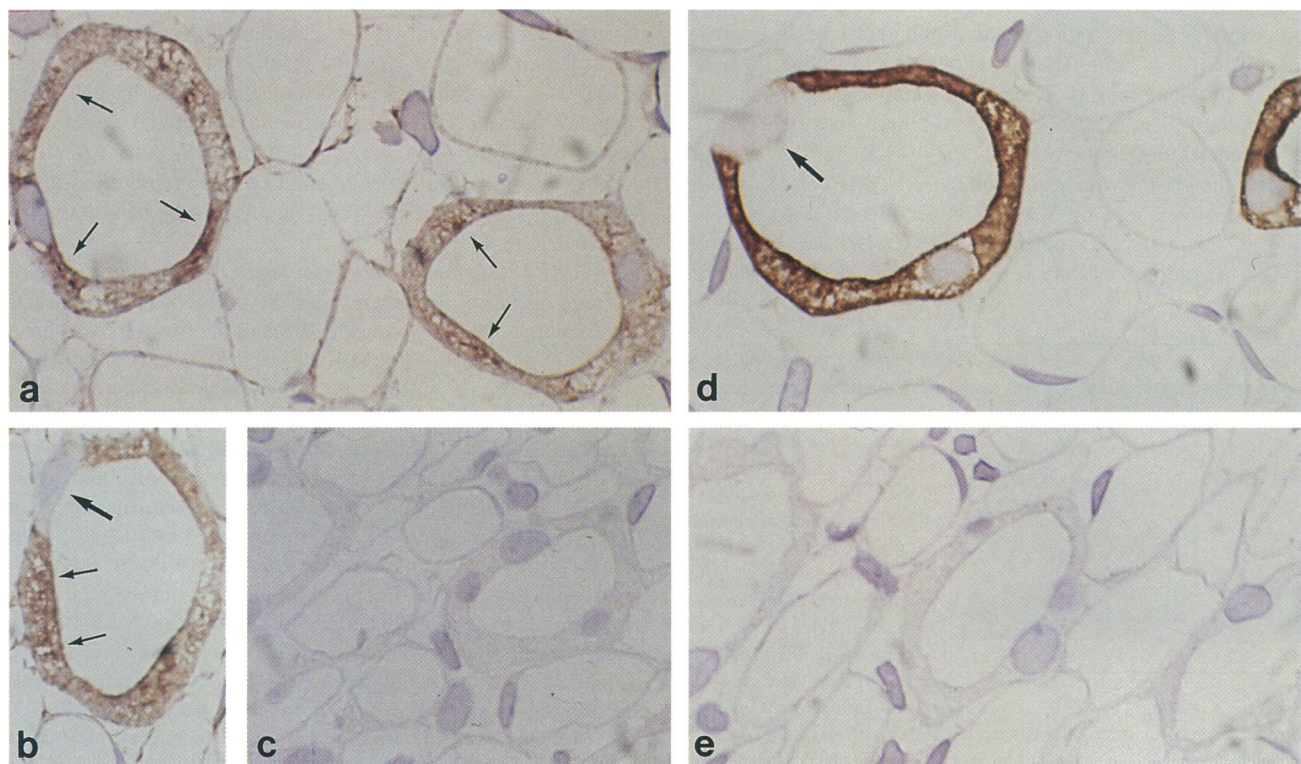


Figure 4. Immunohistochemical localization of VAMP2 (*a-c*) and AQP2 (*d* and *e*) in inner medulla of rat kidney. (*a*) Collecting duct principal cells were heavily labeled with anti-VAMP2 serum, whereas thin limbs and vascular structures exhibit little or no labeling. Within collecting duct principal cells, VAMP2 labeling is predominantly localized to intracellular structures (*arrows*), $\times 1,000$. (*b*) Affinity-purified anti-VAMP also give predominant cytoplasmic labeling of collecting duct principal cells (*small arrows*), whereas collecting duct intercalated cells are not labeled (*large arrow*), $\times 1,000$. (*c*) Control. Use of preimmune serum revealed absence of labeling, $\times 480$. (*d*) Affinity-purified anti-AQP2 exclusively labeled collecting duct principal cells, with labeling of both plasma membranes and intracellular structures. Intercalated cell is without labeling (*arrow*), $\times 1,000$. (*e*) Control. Substitution of primary antibody with nonimmune IgG revealed absence of labeling, $\times 480$.

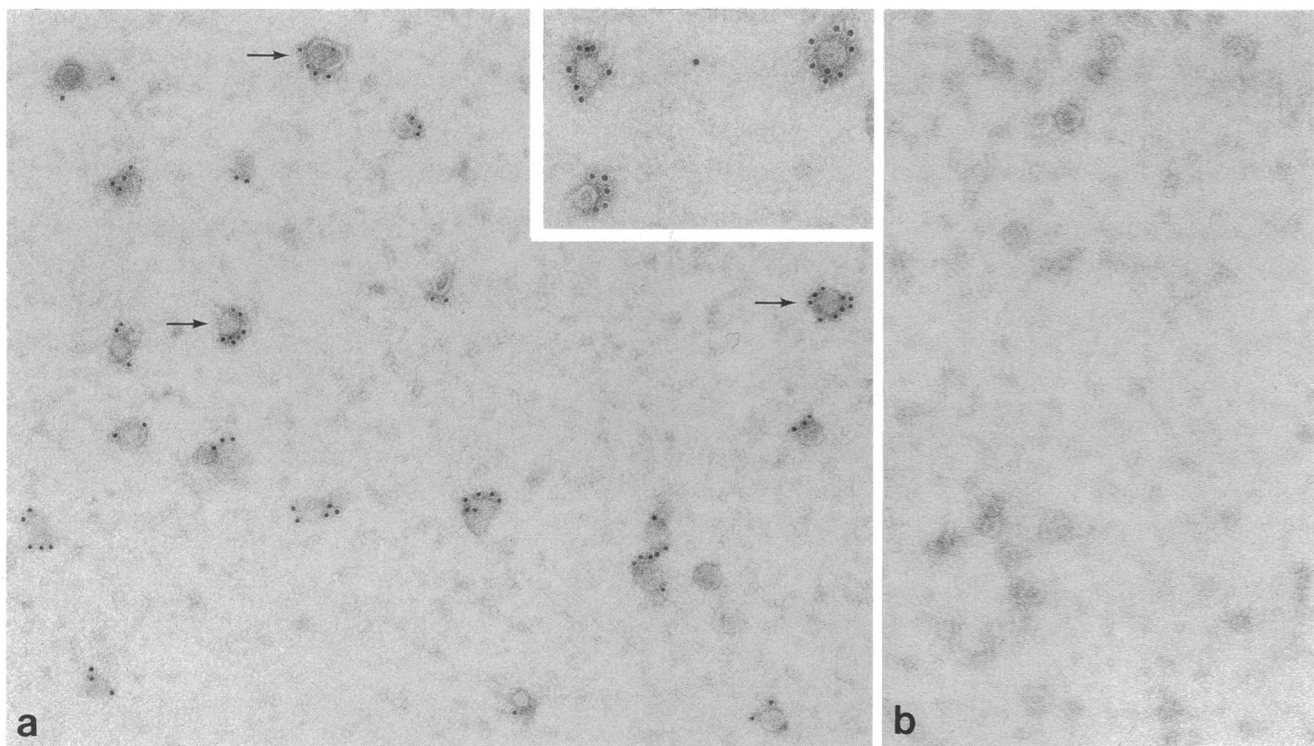


Figure 5. Immunoelectron microscopic labeling of VAMP2 in synaptic vesicles. (a) Synaptic vesicles were labeled with affinity-purified anti-VAMP2 which was visualized with goat anti-rabbit IgG conjugated to 10-nm gold particles. Extensive labeling is seen of almost all synaptic vesicles (arrows), $\times 75,000$. Inset shows labeling at higher magnification, $\times 100,000$. (b) Control labeling using nonimmune IgG, $\times 75,000$.

arrow). Although weak labeling was also seen of thin limbs of the loop of Henle, the predominant labeling was localized to collecting duct principal cells. This labeling pattern was seen with use of antibodies recognizing either the conserved region or the specific region of VAMP2, whereas anti-VAMP1 reveal absence of labeling (not shown). Within the principal cells, the VAMP2 labeling was mainly localized to cytoplasmic components (Fig. 4, a and b). In contrast, the labeling for AQP2 was abundant both in the plasma membrane domain as well as in cytoplasmic vesicles (Fig. 4 d), consistent with previous immunocytochemical and immunoelectron microscopical analyses (3, 4, 8). Corresponding controls were negative (Fig. 4, c and e). Note that, like the anti-VAMP antibody, the anti-AQP2 antibody did not label intercalated cells (Fig. 4 d, arrow).

Colocalization of VAMP2 and AQP2 immunolabeling in the same intracellular vesicles. The immunocytochemical localization of VAMP2 and AQP2 in cytoplasmic vesicles (Fig. 4) was confirmed by single or double immunolabeling for VAMP2 and AQP2 using isolated membrane vesicles. Immunoelectron microscopic localization of VAMP2 and AQP2 was performed using unfixed membrane vesicles placed on grids, followed by negative staining with uranyl acetate. In the synaptic vesicle preparation, intense immunolabeling of VAMP2 was observed (Fig. 5), consistent with previous observations (13), and almost all synaptic vesicles were labeled (Fig. 5). The corresponding immunolabeling control was negative (Fig. 5 b). Application of the same method using membrane vesicles prepared from kidney inner medulla also revealed specific labeling for VAMP2 (Fig. 6). In crude membrane preparations mainly small vesicles were labeled, whereas other membrane vesicles were unlabeled. This is consistent with some vesicles being intracellular vesicles,

whereas others are derived from the plasma membrane and noncollecting duct structures in crude membrane fractions. In membrane fractions enriched for intracellular vesicles, small vesicles were labeled by the VAMP2 antibody, whereas corresponding immunolabeling controls were negative (Fig. 6, b and d).

To determine if VAMP2 colocalizes to the same vesicles which contain AQP2 water channel in their limiting membranes, vesicles were also labeled for AQP2 alone or subjected to double immunolabeling. Heavy labeling of AQP2 in crude membrane fractions was observed in both large and small vesicular structures (Fig. 7 a), consistent with its presence in both plasma membrane and intracellular vesicles. Immunolabeling controls were negative (Fig. 7 b). Double immunolabeling was performed sequentially using two sizes of gold particles conjugated to protein A for visualization of the two polyclonal antibodies, with an interposed blocking step with excess unconjugated protein A. In crude membranes of kidney inner medulla and in a membrane preparation enriched for intracellular vesicles, expression of both VAMP2 and AQP2 was seen in the same vesicles (Fig. 8). Some vesicles were double labeled, whereas others were exclusively labeled for either VAMP2 or AQP2, or were unlabeled.

To support the evidence for colocalization of VAMP2 and AQP2 in the same vesicles, two additional techniques were applied. First we analyzed the double immunogold labeling quantitatively and, in addition, we immunisolated vesicles using anti-VAMP2 antibodies, and then subjected the VAMP-2 immunisolated vesicles to immunoblotting for AQP2.

The quantitative analysis of the double immunolabeling for AQP2 and VAMP2 was performed using immunoelectron mi-

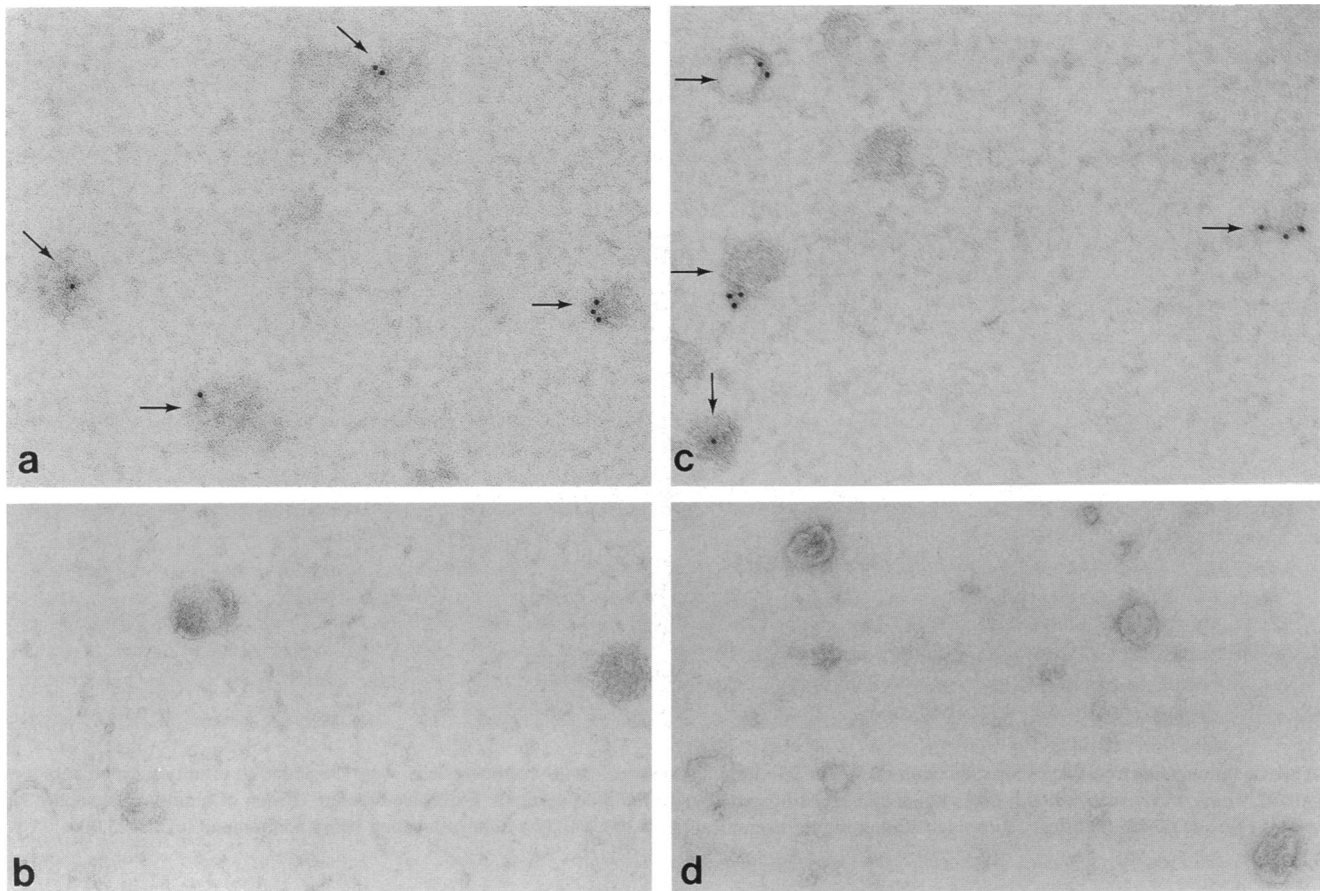


Figure 6. Immunoelectron microscopic labeling of VAMP2 in membrane vesicles from kidney inner medulla labeled with affinity-purified anti-VAMP2 and visualized with goat anti-rabbit IgG conjugated to 10-nm gold particles. (a) Small vesicles in crude membrane fraction were labeled (arrows), $\times 90,000$. (b) Corresponding control using nonimmune IgG revealed absence of labeling, $\times 90,000$. (c) Membrane vesicle preparation enriched for intracellular vesicles was labeled (arrows), $\times 90,000$. (d) Corresponding control using identical concentrations of nonimmune IgG revealed absence of labeling, $\times 70,000$.

scopy of the membrane vesicles from the fraction enriched for intracellular vesicles from kidney inner medulla (as described above). 1,310 vesicles were analyzed after double immunogold labeling and were divided into four groups: vesicles labeled for VAMP2 alone, vesicles labeled for AQP2 alone, vesicles labeled for both, and vesicles not labeled at all. The

results are shown in Table I. To test statistically for colocalization, a χ^2 test was applied using the number of vesicles in each group (Table I). The statistical analysis of the distribution of labeled vesicles revealed a highly significant association of AQP2 and VAMP2 in the same vesicles ($P < 0.0001$).

To confirm presence of both VAMP2 and AQP2 in the

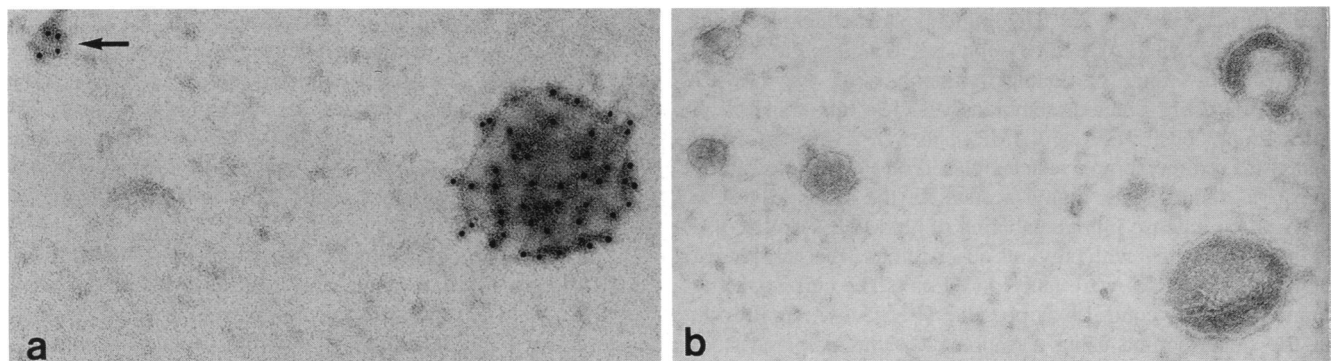


Figure 7. Immunoelectron microscopic labeling of AQP2 in crude membrane vesicles from kidney inner medulla. (a) Large membrane vesicle, presumably plasma membrane-derived, as well as small vesicles are extensively labeled with affinity-purified anti-AQP2 visualized with goat anti-rabbit IgG conjugated to 10-nm gold particles, $\times 100,000$. (b) Corresponding control using nonimmune IgG exhibited no labeling, $\times 76,000$.

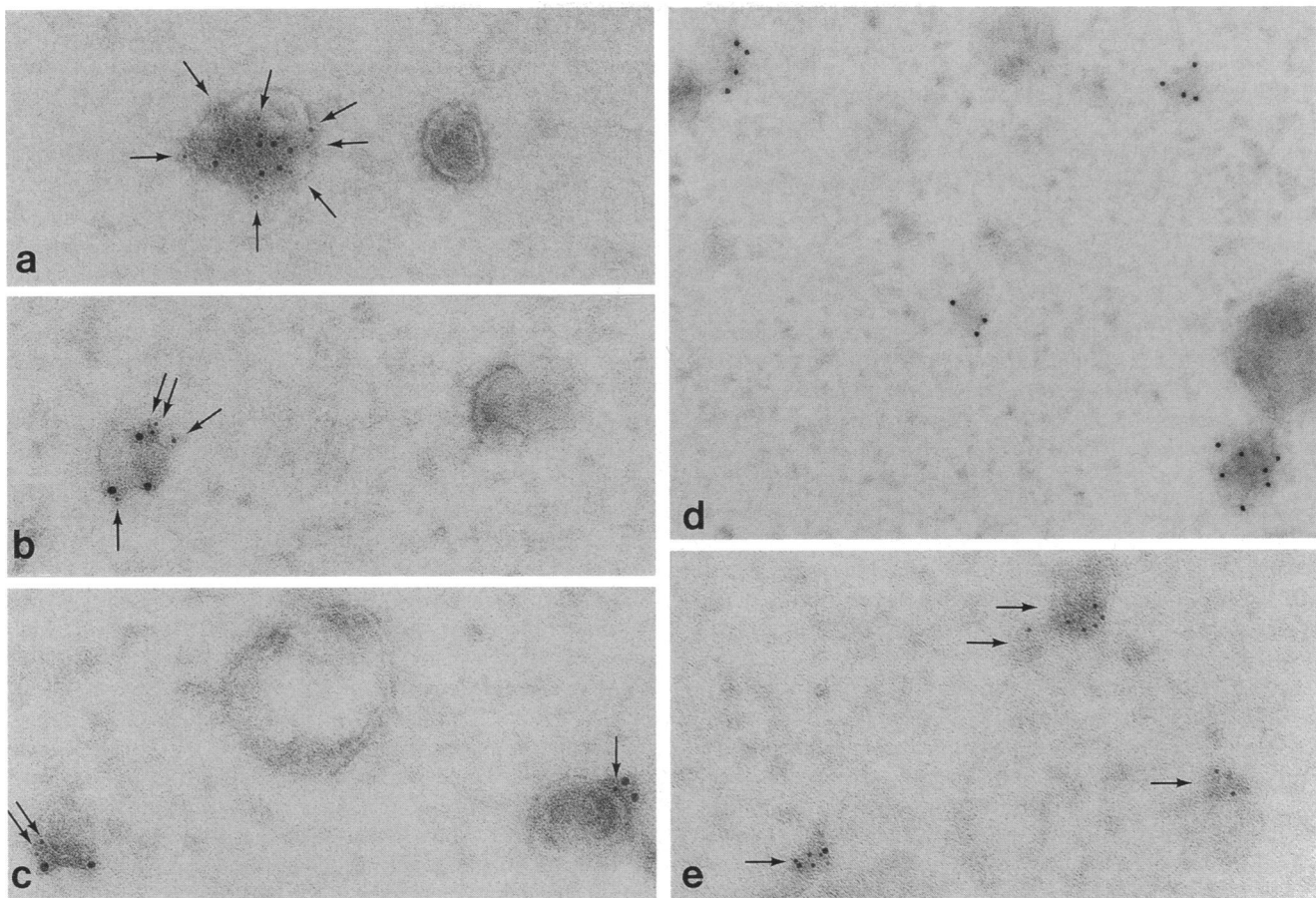


Figure 8. Double immunolabeling of VAMP2 and AQP2 in membrane vesicles from kidney inner medulla. (a) Membrane preparation enriched for intracellular vesicles was first labeled with affinity-purified anti-VAMP2 (visualized with protein A conjugated to 5-nm gold particles) and subsequently blocked with excess protein A before labeling with anti-AQP2 (visualized with protein A conjugated to 10-nm gold particles). Vesicle labeled extensively for AQP2 and VAMP2 (arrows), $\times 110,000$. (b) Immunolabeling prepared identical to that in a, except that the labeling was performed for AQP2 before labeling for VAMP2, $\times 130,000$. (c) Crude membrane fraction from inner medulla subjected to double labeling as described in a. Two small vesicles are labeled for AQP2 and VAMP2 (arrows) whereas large membrane vesicle is unlabeled, $\times 130,000$. (d) Corresponding negative control for VAMP2 double labeling in crude vesicles. Anti-VAMP2 antibody was substituted with nonimmune IgG (5-nm particles) and anti-AQP2 is visualized with 10-nm protein A-gold. Small vesicles were heavily labeled for AQP2 but revealed absence of labeling with 5-nm protein A-gold, $\times 75,000$. (e) Negative control for AQP2 double labeling. Affinity-purified anti-VAMP2 (5-nm protein A-gold) labeled several vesicles. Nonimmune IgG instead of anti-AQP2 revealed almost total absence of labeling (10-nm protein A-gold), $\times 130,000$.

same vesicles, a fraction enriched for intracellular vesicles was subjected to immunoisolation with anti-VAMP2 antibodies (see Methods). Immunoblotting revealed significant AQP2 immunolabeling of both the nonglycosylated and glycosylated forms of AQP2 in the vesicles immunoisolated with VAMP2 antibody

(Fig. 3 C). This confirmed expression of both AQP2 and VAMP2 in the same vesicles. Immunolabeling controls using either nonimmune IgG (not shown) or affinity-purified anti-AQP2 previously reacted with immunizing peptide (Fig. 3 C, lane 3) revealed no labeling of AQP2 bands, whereas IgG was

Table I. Distribution and Labeling Density of Double Immunolabeling for AQP2 and VAMP2 in Intracellular Vesicles from Kidney Inner Medulla

Labeling	AQP2 only	VAMP2 only	AQP2 and VAMP2	None	Total
Number of vesicles*	193	203	153	761	1310
Percentage of vesicles	15 \pm 1	16 \pm 1	12 \pm 1	57 \pm 2	
Labeling density (gold particles/vesicle)	2.5 \pm 0.3	2.1 \pm 0.2	2.6 \pm 0.2 (AQP2) 1.9 \pm 0.2 (VAMP2)	—	

Vesicles were applied to grids and subjected to double immunolabeling for AQP2 and VAMP2 sequentially (see Methods). 1,310 vesicles were analyzed quantitatively. * χ^2 test of distribution of labeled vesicles gave a χ^2 of 67.9, $P < 0.0001$, demonstrating significant colocalization of AQP2 and VAMP2 in the same vesicles.

detected by the secondary antibody. Thus, VAMP2 in kidney collecting duct is, at least partly, localized in a population of small vesicles also expressing AQP2 in their limiting membranes as determined by quantitative immunoelectron microscopy and vesicle immunoisolation, consistent with the view that VAMP2 may play a role in AQP2-vesicle targeting and trafficking.

Discussion

The SNARE hypothesis put forward by Rothman and colleagues (9) proposes that a membrane protein resident in the transport vesicle (the v-SNARE) pairs with its cognate receptor on the target membrane (the t-SNARE). This complex represents the docked state, and subsequent binding by one or more SNAP proteins and NSF is proposed to lead to the formation of a 20S fusion complex. Hydrolysis of ATP by NSF would then cause the fusion of the vesicle and the target membranes, which in the case of the nervous system leads to neurotransmitter release (10, 32). Structurally related yeast proteins are also required for targeting and fusion of transport vesicles with their acceptor compartment in the secretory pathway (for review see reference 32). Thus, intracellular membrane fusion events in different species appear to involve similar mechanisms and use identical or related components. To examine if this vesicle targeting system is involved in regulated trafficking of AQP2-bearing vesicles in the kidney collecting duct in response to vasopressin, we tested if the v-SNAREs VAMP1 or VAMP2 were expressed in the kidney collecting duct. The results demonstrate that: (a) VAMP2, or a VAMP2-like protein, of 18 kD is expressed in kidney inner medulla, whereas VAMP1 is not expressed; (b) the VAMP2 homologue is tetanus toxin sensitive; (c) VAMP2 is found predominantly in subcellular fractions containing intracellular vesicles, with little or no VAMP2 in fractions containing plasma membrane; (d) immunocytochemistry demonstrates VAMP2 immunolabeling mainly in vesicles in principal cells of the collecting duct and absence of VAMP2 in intercalated cells; and (e) VAMP2 is found in AQP2-bearing vesicles, as demonstrated by quantitative double immunolabeling at an electron microscopical level and by vesicle immunoisolation followed by immunoblotting. These results strongly support a role of VAMP2 in vasopressin-regulated vesicular trafficking of AQP2 water channels in the control of body water balance. This extends the role of the vesicle targeting proteins and the SNARE hypothesis to include certain regulatory systems outside the nervous system.

Mechanisms of regulation of AQP2 water channels. Vasopressin regulates both the expression of AQP2 (long-term regulation) and the delivery of AQP2 to the apical plasma membrane in the acute response to vasopressin (short-term regulation). With regard to the long-term regulation, it has been shown that direct or indirect changes in vasopressin levels regulate the expression of AQP2 protein (3, 4, 8, 33). Furthermore, absence of AQP2 has been documented in both primary and acquired forms of diabetes insipidus (4, 7, 8), demonstrating the significance of AQP2 in maintenance of body water balance.

With regard to the short-term regulation, we have shown recently that vasopressin increases the water permeability of collecting duct principal cells by inducing a reversible translocation of AQP2 from intracellular vesicles to the plasma membrane (6). This provided the first direct evidence that vesicular trafficking of AQP2 represents the regulatory mechanism for

the hydroosmotic action of vasopressin. We have subsequently confirmed this by *in vivo* studies demonstrating specific transfer of AQP2 from vesicles to the apical plasma membrane (5), the rate-limiting barrier for transepithelial water reabsorption (34). Thus, both the long-term and the short-term regulation of AQP2 by vasopressin require targeting of AQP2 to the apical plasma membrane. However, the short-term regulated trafficking of AQP2 is apparently superimposed on the long-term adaptation which increases overall AQP2 levels. Based on the extensive evidence for vasopressin-regulated trafficking of AQP2, it became very important to define the molecular apparatus involved in the targeting of AQP2. In this study we demonstrate that AQP2-bearing vesicles express VAMP2, a component of the SNARE receptor complex involved in synaptic vesicle targeting. This strongly suggests that VAMP2 is involved in vasopressin-regulated targeting of AQP2.

VAMP2 expression in kidney inner medulla. Immunoblotting of both crude membrane fractions from kidney inner medulla and inner medullary membrane fractions enriched for intracellular vesicles revealed expression of an 18-kD VAMP2 species. This protein comigrates with VAMP2 from brain vesicles or purified synaptic vesicles. Use of an antibody recognizing the conserved regions of VAMP1 and 2 gave the same result, whereas VAMP1-specific antibodies detected no immunolabeling in kidney inner medulla. Thus, the VAMP homologue expressed in kidney inner medulla is VAMP2 or a closely related VAMP2-like protein. Expression predominantly in the collecting duct is consistent with the observed absence of VAMP2 labeling of crude membranes from kidney cortex (Fig. 1), in which most membrane is obtained from proximal tubules and glomeruli.

The clostridial toxins, tetanus and botulinum toxin, have proven to be important tools in analyzing the expression and function of vesicle-targeting proteins. These toxins are composed of two disulfide-linked polypeptide chains, a heavy chain mediating specific binding to neuronal plasma membranes and a light chain which acts as the neurotoxin. The toxins inhibit neurotransmitter release (35) and have been shown to be Zn²⁺-dependent endopeptidases, having an active zinc binding motif. The amino-terminal part of the toxin light chain is involved in the substrate recognition (31). They act in the neuronal cytosol, specifically cleaving VAMP2. (tetanus toxin and botulinum toxin serotype B, D, F, and G [19, 36, 37]), SNAP-25 (botulinum A and B), or syntaxin (botulinum serotype C1) (for reviews see references 31 and 38). We used both DTT-reduced (nicked) purified whole tetanus toxin and recombinant light chain tetanus toxin in our experiments. Both preparations gave identical results, with complete cleavage of VAMP2 in brain and synaptic vesicles and in membranes from kidney inner medulla (Fig. 2). Tetanus toxin has been shown to cleave VAMP2 specifically at Gln⁷⁶-Phe⁷⁷ resulting in two fragments of ~ 12 and 7 kD (19). Consistent with this, we observed complete cleavage of VAMP2 in brain and synaptic vesicles with no intact VAMP2 left and with presence of an ~ 12 kD hydrolysis product (Fig. 2). Similarly complete cleavage of VAMP2 was observed in the crude membrane fraction and the membrane fraction enriched for intracellular vesicles from kidney inner medulla. The cleavage was complete with no intact VAMP2 remaining, whereas a fragment of ~ 12 kD was barely detectable. The low abundance of the cleaved fragment in the nitrocellulose blotting paper is similar to previous observations (37) and is thought to be due to reduced ability of the fragments to

bind the nitrocellulose membrane during blotting. The tetanus toxin experiments demonstrate the presence of tetanus toxin-sensitive VAMP2, or a VAMP2 homologue, in kidney inner medulla.

Localization of VAMP2 in collecting duct and colocalization in AQP2-bearing vesicles. To examine the subcellular localization of VAMP2 in kidney inner medulla, subcellular fractionation and immunoblotting were performed using a standard protocol of subcellular fractionation (24). The vasopressin-regulated water channel, AQP2, is known to be abundantly expressed in both plasma membrane and intracellular vesicles, and, consistent with this, heavy labeling of AQP2 was observed in both membrane fractions. In contrast, VAMP2 was almost exclusively present in the fraction enriched for intracellular vesicles (Fig. 3). The expression in vesicles was confirmed by immunocytochemistry, revealing a localization predominantly in cytoplasmic vesicles in collecting duct principal cells, with no labeling of intercalated cells (Fig. 4*b*). This was observed by use of both a VAMP2-specific antibody and by use of an antibody recognizing the conserved regions of VAMP1 and 2.

To analyze the expression pattern further, we applied a method described previously for localization of VAMP/synaptobrevin in synaptic vesicles (13). VAMP2 immunolabeling of isolated purified synaptic vesicles revealed abundant labeling of synaptic vesicles (Fig. 5), consistent with previous studies (13). When this method was applied on the membrane fraction enriched for intracellular vesicles from kidney inner medulla, specific labeling of small vesicles was observed (Fig. 6). To provide further evidence for the involvement of VAMP2 in trafficking of AQP2-bearing vesicles, double immunolabeling was performed using kidney inner medullary vesicles. Specific VAMP2 labeling was observed in the same vesicles labeled for AQP2. This was substantiated by quantification of the double labeling (Table I) revealing highly significant association of AQP2 and VAMP2 in the same vesicles. Finally, immunoblotting of vesicles immunisolated with VAMP2 antibodies revealed presence of AQP2 (Fig. 3*C*). All the methods used demonstrate colocalization of the two membrane proteins. Thus, several lines of evidence, including membrane fractionation studies (Fig. 3), immunocytochemistry (Fig. 4), immunoelectron microscopy using both single and double immunolabeling procedures (Figs. 5–8 and Table I), and vesicle immunoisolation (Fig. 3*C*), strongly point to the view that VAMP2 may be involved in vesicle trafficking in the collecting duct and in trafficking of AQP2.

Functional roles of VAMP. Neurotransmitter release from presynaptic nerve terminals occurs by Ca^{2+} -regulated exocytosis of transmitters from synaptic vesicles, which represent a specialized secretory organelle. As described above, the identified synaptic vesicle-associated proteins have specific roles for targeting, docking, and fusion of synaptic vesicles with the plasma membrane. Several lines of evidence suggest a direct role of VAMPs in the exocytic process in neurons. Recently, Hunt et al. (38) demonstrated a significant inhibition of neurotransmitter release subsequent to injection of either botulinum B or a recombinant protein corresponding to the cytoplasmic domain of squid synaptobrevin (VAMP) into squid axons. The inhibition suggests a postdocking role of VAMP in synaptic vesicle fusion (38) and substantiates previous evidence for a role for VAMP in the exocytic release of neurotransmitters.

VAMP homologues have also been shown recently to be expressed in certain nonneuronal tissues, including pancreatic

acinar cell zymogen granules (21) and vesicles carrying the insulin-sensitive glucose-transporter GLUT4 in adipocytes (22). In addition to the known effect of clostridial toxins in neuronal cells, it was shown that tetanus toxin light chain treatment cleaved VAMP2 in pancreatic acinar cell zymogen granules and, importantly, partly inhibited Ca^{2+} -stimulated enzyme secretion. This provided direct support for a role of VAMP in regulated exocytosis in nonneuronal cells. The present results, demonstrating expression of VAMP2 in AQP2-bearing vesicles, strongly suggest a role of VAMP2 in vasopressin-mediated regulation of AQP2 trafficking.

Acknowledgments

The authors thank Trine Møller, Inger Kristoffersen, and Hanne Sidelmann for excellent technical assistance.

Support for this study was provided by The Novo Nordisk Foundation, The Danish Medical Research Council, University of Aarhus Research Foundation, Danish Foundation for the Advancement of Medical Science, Danish Academy of Sciences, the Biomembrane Research Center at University of Aarhus, the Natural Sciences and Engineering Research Council of Canada, and the National Heart, Lung, and Blood Institute.

References

1. Knepper, M. A. 1994. The aquaporin family of molecular water channels. *Proc. Natl. Acad. Sci. USA*. 91:6255–6258.
2. Fushimi, K., S. Uchida, Y. Hara, Y. Hirata, F. Marumo, and S. Sasaki. 1993. Cloning and expression of apical membrane water channel of rat kidney collecting tubule. *Nature (Lond.)*. 361:549–552.
3. Nielsen, S., S. R. DiGiovanni, E. I. Christensen, M. A. Knepper, and H. W. Harris. 1993. Cellular and subcellular immunolocalization of vasopressin-regulated water channel in rat kidney. *Proc. Natl. Acad. Sci. USA*. 90:11663–11667.
4. DiGiovanni, S. R., S. Nielsen, E. I. Christensen, and M. A. Knepper. 1994. Regulation of collecting duct water channel expression by vasopressin in Brattleboro rat. *Proc. Natl. Acad. Sci. USA*. 91:8984–8988.
5. Marples, D., M. A. Knepper, E. I. Christensen, and S. Nielsen. 1995. Redistribution of Aquaporin-2 water channels induced by vasopressin in rat kidney inner medullary collecting duct. *Am. J. Physiol.* In press.
6. Nielsen, S., C. L. Chou, D. Marples, E. I. Christensen, B. K. Kishore, and M. A. Knepper. 1995. Vasopressin increases water permeability of kidney collecting duct by inducing translocation of aquaporin-CD water channels to plasma membrane. *Proc. Natl. Acad. Sci. USA*. 92:1013–1017.
7. Deen, P. M., M. A. Verdijk, N. V. Knoers, B. Wieringa, L. A. Monnens, C. H. van-Os, and B. A. van-Oost. 1994. Requirement of human renal water channel aquaporin-2 for vasopressin-dependent concentration of urine. *Science (Wash. DC)*. 264:92–95.
8. Marples, D., S. Christensen, E. I. Christensen, P. D. Ottosen, and S. Nielsen. 1995. Lithium-induced downregulation of aquaporin-2 water channel expression in rat kidney medulla. *J. Clin. Invest.* 95:1838–1845.
9. Sollner, T., S. W. Whiteheart, M. Brunner, H. Erdjument-Bromage, S. Geromanos, P. Tempst, and J. E. Rothman. 1993. SNAP receptors implicated in vesicle targeting and fusion. *Nature (Lond.)*. 362:318–324.
10. Rothman, J. E. 1994. Mechanisms of intracellular protein transport. *Nature (Lond.)*. 372:55–63.
11. Elferink, L. A., W. S. Trimble, and R. H. Scheller. 1989. Two vesicle-associated membrane protein genes are differentially expressed in the rat central nervous system. *J. Biol. Chem.* 264:11061–11064.
12. Trimble, W. S., D. M. Cowan, and R. H. Scheller. 1988. VAMP-1: a synaptic vesicle-associated integral membrane protein. *Proc. Natl. Acad. Sci. USA*. 85:4538–4542.
13. Baumert, M., P. R. Maycox, F. Navone, P. De-Camilli, and R. Jahn. 1989. Synaptobrevin: an integral membrane protein of 18,000 daltons present in small synaptic vesicles of rat brain. *EMBO (Eur. Mol. Biol. Organ.) J.* 8:379–384.
14. Bennett, M. K., N. Calakos, and R. H. Scheller. 1992. Syntaxin: a synaptic protein implicated in docking of synaptic vesicles at presynaptic active zones. *Science (Wash. DC)*. 257:255–259.
15. Bennett, M. K., J. E. Garcia-Ararras, L. A. Elferink, K. Peterson, A. M. Flemming, C. D. Hazuka, and R. H. Scheller. 1993. The syntaxin family of vesicular transport receptors. *Cell*. 74:863–873.
16. Oyler, G. A., G. A. Higgins, R. A. Hart, E. Battenberg, M. Billingsley,

- F. E. Bloom, and M. C. Wilson. 1989. The identification of a novel synaptosomal-associated protein, SNAP-25, differentially expressed by neuronal subpopulations. *J. Cell Biol.* 109:3039–3052.
17. Sudhof, T. C., M. Baumert, M. S. Perin, and R. Jahn. 1989. A synaptic vesicle membrane protein is conserved from mammals to *Drosophila*. *Neuron* 2:1475–1481.
18. McMahon, H. T., Y. A. Ushkaryov, L. Edelman, E. Link, T. Binz, H. Niemann, R. Jahn, and T. C. Sudhof. 1993. Cellubrevin is a ubiquitous tetanus-toxin substrate homologous to a putative synaptic vesicle fusion protein. *Nature (Lond.)* 364:346–349.
19. Schiavo, G., F. Benfenati, B. Poulain, O. Rossetto, P. Poverino-de-Laureto, B. R. DasGupta, and C. Montecucco. 1992. Tetanus and botulinum-B neurotoxins block neurotransmitter release by proteolytic cleavage of synaptobrevin. *Nature (Lond.)* 359:832–835.
20. Trimble, W. S., T. S. Gray, L. A. Elferink, M. C. Wilson, and R. H. Scheller. 1990. Distinct patterns of expression of two VAMP genes within the rat brain. *J. Neurosci.* 10:1380–1387.
21. Gaisano, H. Y., L. Sheu, J. K. Foskett, and W. S. Trimble. 1994. Tetanus toxin light chain cleaves a vesicle-associated membrane protein (VAMP) isoform 2 in rat pancreatic zymogen granules and inhibits enzyme secretion. *J. Biol. Chem.* 269:17062–17066.
22. Cain, C. C., W. S. Trimble, and G. E. Lienhard. 1992. Members of the VAMP family of synaptic vesicle proteins are components of glucose transporter-containing vesicles from rat adipocytes. *J. Biol. Chem.* 267:11681–11684.
23. Trimble, W. S. 1993. Analysis of the structure and expression of the VAMP family of synaptic vesicle proteins. *J. Physiol. (Paris)* 87:107–115.
24. Jorgensen, P. L. 1974. Isolation of (Na⁺ K⁺)-ATPase. *Methods Enzymol.* 32:277–290.
25. Lowry, O. H., N. J. Rosebrough, A. L. Farr, and R. J. Randall. 1951. Protein measurement with the Folin phenol reagent. *J. Biol. Chem.* 193:265–275.
26. Huttner, W. B., W. Schiebler, P. Greengard, and P. De-Camilli. 1983. Synapsin I (protein I), a nerve terminal-specific phosphoprotein. III. Its association with synaptic vesicles studied in a highly purified synaptic vesicle preparation. *J. Cell Biol.* 96:1374–1388.
27. Nielsen, S., B. Smith, E. I. Christensen, M. A. Knepper, and P. Agre. 1993. CHIP28 water channels are localized in constitutively water-permeable segments of the nephron. *J. Cell Biol.* 120:371–383.
28. Nielsen, S., B. L. Smith, E. I. Christensen, and P. Agre. 1993. Distribution of Aquaporin CHIP in secretory and resorptive epithelia and capillary endothelia. *Proc. Natl. Acad. Sci. USA.* 90:7275–7279.
29. Smith, B. L., R. Baumgarten, S. Nielsen, D. Raben, M. L. Zeidel, and P. Agre. 1993. Concurrent expression of erythroid and renal aquaporin CHIP and appearance of water channel activity in perinatal rats. *J. Clin. Invest.* 92:2035–2041.
30. Tokuyasu, K. T. 1986. Application of cryoultramicrotomy to immunocytochemistry. *J. Microsc. (Oxf.)* 143:139–149.
31. Rossetto, O., G. Schiavo, C. Montecucco, B. Poulain, F. Deloye, L. Lozzi, and C. C. Shone. 1994. SNARE motif and neurotoxins. *Nature (Lond.)* 372:415–416.
32. Ferro-Novick, S., and R. Jahn. 1994. Vesicle fusion from yeast to man. *Nature (Lond.)* 370:191–193.
33. Hayashi, M., S. Sasaki, H. Tsuganezawa, T. Monkawa, W. Kitajima, K. Konishi, K. Fushimi, F. Marumo, and T. Saruta. 1994. Expression and distribution of aquaporin of collecting duct are regulated by vasopressin V2 receptor in rat kidney. *J. Clin. Invest.* 94:1778–1783.
34. Flamion, B., and K. R. Spring. 1990. Water permeability of apical and basolateral cell membranes of rat inner medullary collecting duct. *Am. J. Physiol.* 259:F986–F999.
35. Huttner, W. B. 1993. Snappy exocytosis. *Nature (Lond.)* 365:104–105.
36. Schiavo, G., B. Poulain, O. Rossetto, F. Benfenati, L. Tauc, and C. Montecucco. 1992. Tetanus toxin is a zinc protein and its inhibition of neurotransmitter release and protease activity depend on zinc. *EMBO (Eur. Mol. Biol. Organ.) J.* 11:3577–3583.
37. Link, E., L. Edelman, J. H. Chou, T. Binz, S. Yamasaki, U. Eisel, M. Baumert, T. C. Sudhof, H. Niemann, and R. Jahn. 1992. Tetanus toxin action: inhibition of neurotransmitter release linked to synaptobrevin proteolysis. *Biochem. Biophys. Res. Commun.* 189:1017–1023.
38. Hunt, J. M., K. Bommert, M. P. Charlton, A. Kistner, E. Habermann, G. J. Augustine, and H. Betz. 1994. A post-docking role for synaptobrevin in synaptic vesicle fusion. *Neuron* 12:1269–1279.